

# SUBSTRUCTURAL IDENTIFICATION OF BRIDGE — A FFT-BASED SPECTRAL ANALYSIS

Zheng-Kuan LEE<sup>1</sup> and Chin-Hsiung LOH<sup>2</sup>

<sup>1</sup>Graduate student, Dept. of Civil Eng., National Taiwan University, (Taipei, Taiwan, R.O.C.)

<sup>2</sup>Member of JSCE, Professor, Dept. of Civil Eng., National Taiwan University, (Taipei, Taiwan, R.O.C.)

The purpose of this paper is to use the seismic response data of one 5-span continuous box-girder bridge to identify the dynamic characteristics of the system from different earthquake loading. The spectral finite element method was used by considering the flexural wave in beam to form the dynamic stiffness matrix of the substructure. Through matrix condensation the interior nodal displacement can be expressed in terms of the boundary nodal displacements. The identification was performed by using the recorded nodal displacement of the bridge to identify the  $EI$ -value and damping factor  $\eta$  of the substructure. Three seismic event data sets were used from the bridge strong motion instrumentation array. It is found that the identified  $EI$ -values are very stable even for different intensity of earthquake loading while the damping value may change from seismic event to event.

*Key Words:* system identification, spectral theory, wave-motion

## 1. INTRODUCTION

There has been a considerable demand for more accurate techniques to detect and locate damage in large structures. Damage will cause the stiffness distribution in the structure to change, which may be detected by measuring its dynamic response. Among the dynamic response analysis, reference<sup>1</sup> used the natural frequencies only to detect damage. In reference<sup>2</sup>, used is made of the property that the curvature of the mode shapes increases at the location of the damage. In reference<sup>3</sup>, damage detection was carried out by two successive procedures. At the beginning, the eigensolution of the structure is identified using a modal parameter identification technique and the system response. Then, the identified eigensolution is used together with properties of the eigenvalue problem to detect the damage components.

Most civil engineering structures such as multi-story buildings and bridges accumulate damage gradually during their service lives.

From the viewpoint of serviceability and safety of structures, an important issue is the identification and detection of structural damage, particularly after earthquakes. In this regards, there has been many noticeable research works using the system identification techniques (SI) to study the dynamic response of structures subjected to earthquake excitations (e.g., Ref.<sup>4,5,6,7</sup>). The aim is to identify structural parameters (e.g., stiffness), which are then compared with the original design values, thereby providing a means to locate and quantify the structural changes due to deterioration or damage.

In general, the transient response of civil engineering structures can be obtained by using the methodology of finite elements combined with a suitable scheme to solve the equation of motion in time domain. An approach similar in style to that of the finite element method (FEM) of analysis is the spectral representation. The spectral formulation begins with the equation of motion of the beam including the inertia term<sup>8</sup>. This spectral approach to

dynamic problems temporarily removes time from the description that the effect of damping can easily be incorporated by changing the spectrum relation. The dynamic stiffness of the beam element can be established in spectral representation. If the response is known at some location the inverse problems can be performed. Application of the spectral finite element method to the parametric identification of frames using transient data had been employed through simulation<sup>9)</sup>. The purpose of this paper is to use the spectral finite element method to the identification of bridge dynamic characteristics from seismic response data. Research work will be concentrated on the substructural identification.

## 2. SEISMIC RESPONSE DATA OF NEW-LIAN RIVER BRIDGE

The New-Lian River Bridge (NLRB), a continuous five-span prestressed box-girder bridge, is located at the northeast coast of Taiwan. This bridge was instrumented in November 1994 by Central Weather Bureau. This instrumentation comprises single-axis, two-axes and triaxial force-balanced accelerometers with 16-bit resolution which makes the apparatus capable of recording high-resolution ground motion and structural response within  $\pm 2g$  over

a nominal frequency range of 0 to 100Hz and with a pre-event and post-event memory. A total of 24 strong motion accelerometers along its deck, at its abutments and a nearby free-field location (as shown in Fig.1). Most of these instruments were triggered during Feb. 23, 1995, June 25, 1995 and March 5, 1996 earthquakes, providing one of the most extensive array of strong motion measurements. Table 1 shows the recorded maximum acceleration from the recorded accelerograms. The event of June 25, 1995 earthquake induced significant response at some of the measurement points. Fig.2 shows some recorded acceleration from these three events.

Preliminary analysis on the seismic response data of the bridge had been discussed<sup>10)</sup>. Using ARX-model for case of multi-inputs/single output (multi-inputs denotes the multiple-supported excitations from different abutments) the identified first two dominant vibration frequencies in transverse direction is 9.04rad/sec and 12.5rad/sec, respectively. Except the global system identification, substructural system identification was also applied. Using lumped mass model a bridge-girder substructure shown in Fig.3 is selected as a substructural system. The motion equation in transverse direction of mass  $m_i$  (mass lumped at the top of the pier) can be formulated:

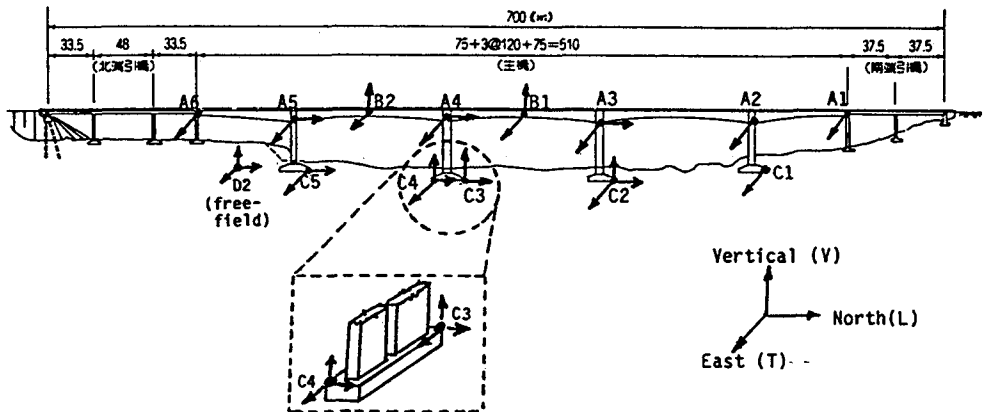
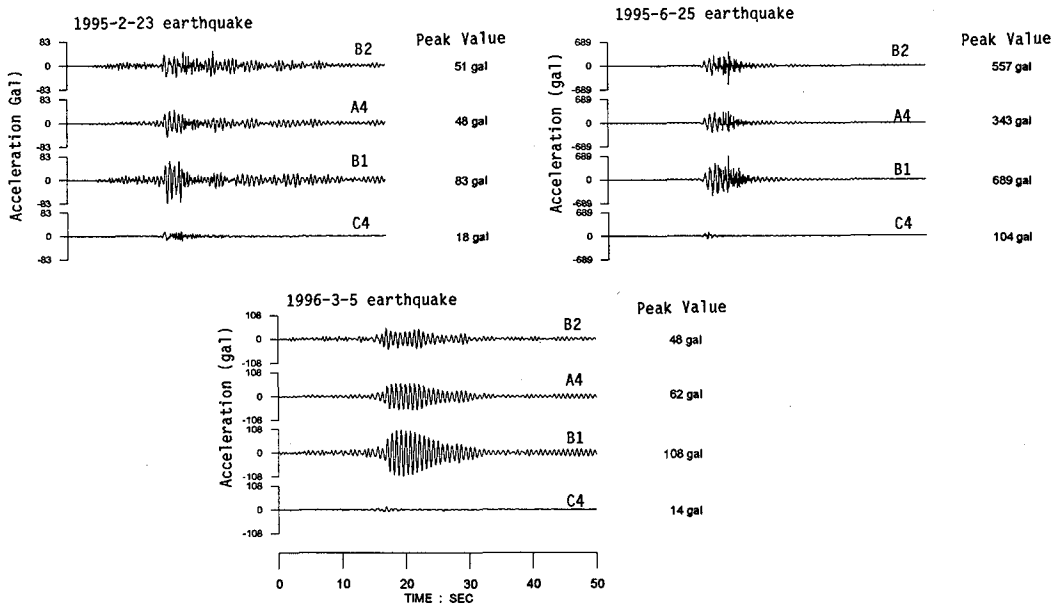


Fig.1 Instrumentation layout at New-Lian River Bridge.  
The motion in the east direction represents the transverse motion.

**Table 1** Recorded maximum peak acceleration from instrumentations at Oew-Lian River Bridge for 1995-2-23, 1995-6-25, and 1996-3-5 earthquakes.

	Earthquake : Feb. 23, 1995 M = 5.77 D = 21.7 km			Earthquake : June 25, 1995 M = 6.50 D = 39.9 km			Earthquake : March 5, 1996 M = 6.4 D = 28 km		
	EW	NS	VR	EW	NS	VR	EW	NS	VR
C1	16	--	--	120	--	--	9.4	--	--
C2	19	13.4	8.3	125	131	48	14.3	8.2	4.8
C3	--	--	9.5	--	107	58	--	13.9	4.7
C4	18	12.7	8.7	104	101	40	14.07	10.63	4.3
C5	15	15.1	--	145	78	--	11.68	--	--
A1	58	--	--	511	--	--	23.4	--	--
A2	28	--	--	188	--	--	24.6	--	--
A3	51	19.2	--	381	212	--	84.5	23.6	--
A4	48	--	--	343	166	--	61.8	24.2	--
A5	43	14.9	--	223	201	--	28.5	--	--
A6	86	--	--	693	--	--	31.5	--	--
B1	83	--	54	689	--	960	107.5	--	41.6
B2	51	--	60	557	--	521	48.5	--	50.5

Unit: Gal  
EW: Corresponding to transverse direction  
NS: Corresponding to longitudinal direction



**Fig.2** Part of the recorded acceleration in transverse direction at station B2, A4, B1 and C4 from the New-Lian River Bridge strong motion instrumentation for three different earthquakes.

$$\begin{aligned}
 & m_i \ddot{u}_i + c_i \dot{u}_i + k_i u_i \\
 & = -m_i \ddot{u}_g(t) \\
 & - c_{i+1} (\dot{u}_i - \dot{u}_{i+1}) - k_{i+1} (u_i - u_{i+1}) \\
 & - c_{i-1} (\dot{u}_i - \dot{u}_{i-1}) - k_{i-1} (u_i - u_{i-1}) \quad (1)
 \end{aligned}$$

where  $k_i$  and  $c_i$  are the stiffness and damping of bridge pier in transverse direction,  $k_{i+1}$  and  $c_{i+1}$  are the girder stiffness and damping between mass  $i$  and mass  $i + 1$ ,  $k_{i-1}$  and  $c_{i-1}$  are the girder stiffness and damping between mass  $i$  and mass  $i - 1$ . In Eq. (1)  $u_{i-1}$ ,  $u_i$  and  $u_{i+1}$  are recorded bridge motion at locations  $i - 1$ ,  $i$  and  $i + 1$  during earthquake.

Time domain identification scheme, such as Kalman filter technique, can be used to identify the modal parameters of the substructural system (i.e.,  $c_i/m_i$ ,  $k_i/m_i$ ,  $c_{i-1}/m_i$ ,  $k_{i-1}/m_i$ ,  $c_{i+1}/m_i$  and  $k_{i+1}/m_i$ ). Basically it is similar to use the shear type model between two lumped masses. **Table 2** shows the estimated stiffness and damping of the NLRB from the data of February 23, 1995 earthquake. The result indicates the identified equivalent stiffness and damping of the substructure between two consecutive measurement points. Difficulty may raise if more elements are used in the model between two consecutive measurements. An approach from the view point of spectral finite element method provides more powerful on the formulation of dynamic problems.

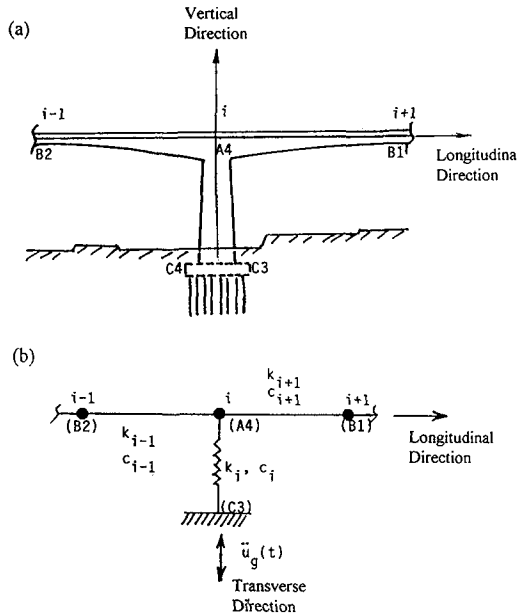


**Fig.3** (a) A bridge-girder substructure system, (b) lumped mass model of the bridge-girder system for motion in transverse direction.

**Table 2** Estimated modal parameters from 1995-2-23 earthquake of the T-section of New-Lian River Bridge (Pier: A4-C4, Girder A4-B2, and Girder: A4-B1).

Feb. 23, 1995 earthquake – Transverse direction		
Pier: A4-C4 section	Girder: A4-B2 section	Girder: A4-B1 section
$K_i/m_i = 91.33$	$K_{i-1}/m_i = 75.473$	$K_{i+1}/m_i = 74.459$
$C_i/m_i = 0.8407$	$C_{i-1}/m_i = 0.8889$	$C_{i+1}/m_i = 0.7395$

### 3. SPECTRAL ANALYSIS OF FLEXURAL WAVES IN BEAMS

Consider the beam element to have constant properties along its length, then the equation of motion (neglecting the rotational inertia term  $\rho I \ddot{\phi}$ ) can be written in the form

$$EI \frac{\partial^4 v(x, t)}{\partial x^4} + \eta \frac{\partial v(x, t)}{\partial t} + \rho A \frac{\partial^2 v(x, t)}{\partial t^2} = 0 \quad (2)$$

where  $\rho A$  is the mass density per unit length of the beam. The displacements are given by their spectral representation as:

$$v(x, t) = \sum_n \hat{v}_n(x, \omega_n) e^{i\omega_n t} \quad (3)$$

The spectral components,  $\hat{v}_n$ , satisfy the following equation of motion

$$EI \frac{d^4 \hat{v}_n}{dx^4} - (\omega_n^2 \rho A - i\omega_n \eta) \hat{v}(x, \omega_n) = 0 \quad (4)$$

Giving the general solution for the deflection curve as

$$\hat{v}_n(x, \omega_n) = C_n e^{-ik_n x} + D_n e^{-k_n x} + E_n e^{-ik_n(L-x)} + F_n e^{-k_n(L-x)} \quad (5)$$

where

$$k_n = \left[ (\omega_n^2 \rho A - i\omega_n \eta) / EI \right]^{1/4}$$

and  $L$  is the length of the beam element. The first two terms are appropriate to wave moving in the plus direction and the second two terms to backward-moving waves.

Assume that there are no external loads applied between two ends of the beam element (between node 1 and node 2), as shown in **Fig.4**. At each node, there are two essential beam actions, namely, the bending moment and shear force. The corresponding nodal degree of freedom are the rotation  $\phi(x, t)$  and the vertical displacement  $v(x, t)$ . Since the beam element is a two-node system, then the stiffness matrix is of order  $4 \times 4$  because there must be two degree-of-freedom at each node. The matrix,  $[\hat{G}]$ , is setup by first relating the coefficients in Eq. (5) to the nodal displacements as

$$\{C_n, D_n, E_n, F_n\}^T = [\hat{G}] \{\hat{v}_{1n}, \hat{\phi}_{1n}, \hat{v}_{2n}, \hat{\phi}_{2n}\}^T \quad (6)$$

where  $\hat{v}_{in}$  and  $\hat{\phi}_{in}$  ( $i = 1, 2$ ) denote the nodal vertical displacement and nodal rotation at node  $i$ . Since the bending moment and shear force are related to the deflection curve

$$M(x, \omega_n) = EI \frac{\partial^2 \hat{v}(x, \omega_n)}{\partial x^2} \quad (7)$$

$$\text{and } V(x, \omega_n) = -EI \frac{\partial^3 \hat{v}(x, \omega_n)}{\partial x^3}$$

Further, these member force values and the nodal force values are related by

$$\begin{aligned} V_{1n} &= V(0, \omega_n), \quad M_{1n} = M(0, \omega_n) \\ V_{2n} &= V(L, \omega_n), \quad M_{2n} = M(L, \omega_n) \end{aligned} \quad (8)$$

Defining the nodal forces and moments and the corresponding generalized nodal displacements as column matrices, the equilibrium equation between nodal responses and nodal forces can be obtained:

$$\begin{Bmatrix} V_{1n} \\ M_{1n} \\ V_{2n} \\ M_{2n} \end{Bmatrix} = [K]_{4 \times 4} \begin{Bmatrix} \hat{v}_{1n} \\ \hat{\phi}_{1n} \\ \hat{v}_{2n} \\ \hat{\phi}_{2n} \end{Bmatrix} \quad (9)$$

where  $[K]$  is the dynamic stiffness matrix of beam element in spectral representation. Through assembling the dynamic stiffness of beam elements the stiffness matrix of substructure can be constructed.

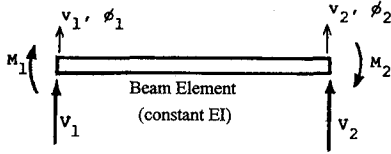


**Fig.4** Nodal loads and degree of freedom of beam element (consider only flexural deformation).

#### (1) Identification of Substructure

The dynamic structural stiffness matrix is assembled in a completely analogous way to that used for the static stiffness. That is, the elements can be assembled into structural system form as

$$[\hat{K}] \{\hat{u}\} = \{\hat{P}\} \quad (10)$$

where  $\{\hat{P}\}$  is the nodal load of the substructure system in frequency domain. If the nodal

displacement vector  $\{\hat{u}\}$  is solved at each frequency, then its time behavior is reconstructed simply by using the FFT inverse. From the system identification point of view the  $EI$ -value and  $\eta$ -value of beam element are unknown if only the flexural waves in beam are considered. Parametric identification of the frame member can be formulated as the optimization problem:

Minimize  $J$

$$= \left\| \left\{ \sum_{n=1}^m [\hat{K}(\omega_n, \hat{s})]^{-1} \{\hat{P}(\omega_n)\} \right\} - F \{u(t)\} \right\|^2 \quad (11)$$

where  $F(\cdot)$  denotes the Fourier transformation of nodal displacement  $u(t)$  and  $\hat{s}$  is the vector of unknown parameters (such as  $EI$  and  $\eta$  values) and  $|\cdot|$  denotes the absolute value of complex value.  $m$  is the number of frequencies to be included. Any nonlinear optimization program, such as Gauss-Newton method, can solve the problem and estimate the model parameters.

#### 4. SUBSTRUCTURAL IDENTIFICATION OF A 5-SPAN CONTINUOUS BRIDGE

Based on the above discussion on the dynamic stiffness of a uniform beam, the assembly of the dynamic stiffness from a specified substructure and the application of the present method to seismic response data of a bridge are discussed. It has to be pointed out that not all the information in the displacement vector  $\{\hat{u}\}$  and force vector  $\{\hat{P}\}$  can be measured directly. Stiffness condensation should be applied to match the degree of freedom where measurements can be obtained. Application of the spectral beam element to this bridge for the purpose of identification was discussed. Consider the substructural system of the bridge as shown in Fig.3a, the complete substructural system can be divided into five beam elements. Four elements are assumed in the two overhanging girder and one element is assumed for the bridge pier. Because the variation of the girder cross section it is assumed that two elements are used in each of the overhanging girder with different  $EI$  value; as shown in Fig.5a.

(b) Girder Substructure

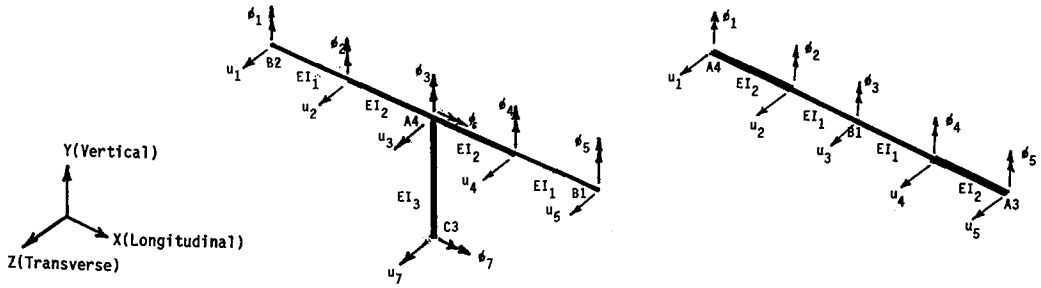


**Fig.5** (a) Pier-girder substructural system (B2-A4-B1). The nodal displacements are indicated and three different  $EI$ -values of beam element are assumed.  
(b) Girder substructural system (A4-B1-A3).

### (1) Formulation

Consider the pier-girder (T-section) substructure. The dynamic stiffness of the substructure in transverse direction should be constructed first. Based on Eq. (10), the nodal force and displacement relationship is shown as Eq. (12). In Eq. (12),  $\hat{u}_1$ ,  $\hat{u}_3$ ,  $\hat{u}_5$ ,  $\hat{u}_7$  and  $\hat{\phi}_7$  can be obtained directly from the measurement.  $\hat{\phi}_1$ ,  $\hat{\phi}_3$  and  $\hat{\phi}_5$  can not be measured directly but can be calculated from:  $\phi(x, t) = du(x, t)/dx$ . The bridge deck displacement in transverse direction,  $u(x, t)$ , can be obtained from Spline approximation by requiring that  $u(x_i, t)$  be the recorded motion along the bridge deck in transverse direction at location " $x_i$ ". Condensation must be performed by describing the internal nodal deformation in terms of the boundary nodal deformation. In this example, there is no external load acts at nodal points 2, 3 and 4,

the nodal forces and moments are described as zero, i.e.,  $\hat{V}_2, \hat{M}_2, \hat{V}_3, \hat{M}_3, \hat{V}_4, \hat{M}_4$  are all zeros. The boundary nodal forces are  $\hat{V}_1, \hat{M}_1, \hat{V}_5, \hat{M}_5, \hat{V}_7$  and  $\hat{M}_7$ . Among them  $\hat{M}_7$  is assumed as zero because a hinge support was assumed at the bottom of the bridge pier. This assumption was based on the identification result of pier stiffness “ $k$ ” from seismic response data using lumped mass model ( $k = 5.16 \times 10^8$  N/m) and also on the calculated pier stiffness from finite element model ( $k = 4.21 \times 10^8$  N/m). The identification result and the design finite element model both have a consistent pier stiffness if hinge support was assumed at the bottom of the pier (Ref.<sup>10</sup>). Since the forces at the boundary of the substructure are unknown, then Eq. (12) can be rearranged by separating interior nodes and exterior nodes in the following form:

[illegible]

$$\begin{Bmatrix} \hat{V}_2 \\ \hat{M}_2 \\ \hat{V}_3 \\ \hat{M}_3 \\ \hat{V}_4 \\ \hat{M}_4 \\ \hat{M}_7 \\ \hat{V}_1 \\ \hat{M}_1 \\ \hat{V}_5 \\ \hat{M}_5 \\ \hat{M}_6 \\ \hat{V}_7 \end{Bmatrix} = \begin{bmatrix} B & A \\ (7 \times 7) & (7 \times 6) \\ \hline C & D \\ (6 \times 7) & (6 \times 6) \end{bmatrix} \begin{Bmatrix} \hat{u}_2 \\ \hat{\phi}_2 \\ \hat{u}_3 \\ \hat{\phi}_3 \\ \hat{u}_4 \\ \hat{\phi}_4 \\ \hat{\phi}_7 \\ \hat{u}_1 \\ \hat{\phi}_1 \\ \hat{u}_5 \\ \hat{\phi}_5 \\ \hat{\phi}_6 \\ \hat{u}_7 \end{Bmatrix} \quad (13)$$

Partition the matrix in Eq. (13) is based on the separation of the boundary nodal points from internal nodal points of the substructure. It is also assumed that  $\hat{\phi}_6$  is equal to zero for this case which means  $\hat{M}_6$  must be provided in order to have  $\hat{\phi}_6 = 0$  (no rotation on bridge deck). Because of this assumption  $\hat{M}_6$  is prescribed as the external moment and assigned it as external load to prevent rotation. Then the nodal force of the internal nodes can be extracted from Eq. (13) and set to zero because of no external loads:

$$\begin{Bmatrix} \hat{V}_2 \\ \hat{M}_2 \\ \hat{V}_3 \\ \hat{M}_3 \\ \hat{V}_4 \\ \hat{M}_4 \\ \hat{M}_7 \end{Bmatrix} = \begin{bmatrix} B \\ (7 \times 7) \end{bmatrix} \begin{Bmatrix} \hat{u}_2 \\ \hat{\phi}_2 \\ \hat{u}_3 \\ \hat{\phi}_3 \\ \hat{u}_4 \\ \hat{\phi}_4 \\ \hat{\phi}_7 \end{Bmatrix} + \begin{bmatrix} A \\ (7 \times 6) \end{bmatrix} \begin{Bmatrix} \hat{u}_1 \\ \hat{\phi}_1 \\ \hat{u}_5 \\ \hat{\phi}_5 \\ \hat{\phi}_6 \\ \hat{u}_7 \end{Bmatrix} = \{0\} \quad (14)$$

It has been pointed out that  $M_7$  is also assumed to be zero in this study because the stiffness of the pier under such assumption is much more consistent with the design value. Since there is no external load at the internal

nodes, then Eq. (14) can be set to zero, so the internal nodal displacement can be calculated and expressed in terms of the boundary nodal displacement:

$$\begin{Bmatrix} \hat{u}_2 \\ \hat{\phi}_2 \\ \hat{u}_3 \\ \hat{\phi}_3 \\ \hat{u}_4 \\ \hat{\phi}_4 \\ \hat{\phi}_7 \end{Bmatrix} = -[B]^{-1}[A] \begin{Bmatrix} \hat{u}_1 \\ \hat{\phi}_1 \\ \hat{u}_5 \\ \hat{\phi}_5 \\ \hat{\phi}_6 \\ \hat{u}_7 \end{Bmatrix} = \begin{bmatrix} G \\ (7 \times 6) \end{bmatrix} \begin{Bmatrix} \hat{u}_1 \\ \hat{\phi}_1 \\ \hat{u}_5 \\ \hat{\phi}_5 \\ \hat{\phi}_6 \\ \hat{u}_7 \end{Bmatrix} \quad (15)$$

The  $[B]$  matrix and  $[A]$  matrix in Eq. (15) contain unknown parameters of the spectral elements ( $EI$  value and  $\eta$  value of element) and  $[G]$  matrix is equal to  $-[B]^{-1}[A]$ . It is also a frequency dependent matrix with unknown parameters. The displacement vector on the right hand side of Eq. (15) is a known vector because the boundary displacement and rotation can be obtained from the records of bridge instrumentation. Since one of the internal nodal displacement,  $u_3(t)$  or  $\hat{u}_3(\omega)$  in frequency domain, can also be obtained directly from the strong motion instrumentation, the optimization problem for this particular substructure can be formulated in frequency domain:

$$\begin{aligned} \text{Minimize } J &= \int_0^\infty |\hat{u}_3(\omega)|^2 d\omega \\ &- \left( G_{31} \hat{u}_1(\omega) + G_{32} \hat{\phi}_1(\omega) + G_{33} \hat{u}_5(\omega) \right. \\ &\quad \left. + G_{34} \hat{\phi}_5(\omega) + G_{35} \hat{\phi}_6(\omega) + G_{36} \hat{u}_7(\omega) \right)^2 d\omega \end{aligned} \quad (16)$$

where “ $\hat{\cdot}$ ” denotes the Fourier transform of the nodal displacement. The nodal displacement, such as  $\hat{\phi}_1$  and  $\hat{\phi}_5$  in Eq. (16), may be obtained from the spline approximation of bridge deck deformation in transverse direction as discussed before.

## (2) Results of Identification

To illustrate the method, the same pier-girder substructure of the bridge (the T-section includes two over hang girders and the pier system) will be analyzed, as shown in Fig.5. Table 3 shows the identified  $EI$ -value and  $\eta$  value between points B2 and A4, C4 and A4, and A4 and B1. The identified  $EI$ -value for each element are quite similar even for different seismic event. The  $\eta$ -value is larger for the case of 1995-6-25 earthquake. This is quite reasonable because for the 1995-6-25 earthquake larger structural responses were measured. From Eq. (15) the unknown interior nodal displacement can also be retrieved. From Eq. (13) the boundary forces (bending moment and shear force) can also be retrieved as follows:

$$\begin{Bmatrix} \hat{V}_1 \\ \hat{M}_1 \\ \hat{V}_5 \\ \hat{M}_5 \\ \hat{M}_6 \\ \hat{V}_7 \end{Bmatrix} = \begin{bmatrix} C \\ (6 \times 7) \end{bmatrix} \begin{Bmatrix} \hat{u}_2 \\ \hat{\phi}_2 \\ \hat{u}_3 \\ \hat{\phi}_3 \\ \hat{u}_4 \\ \hat{\phi}_4 \\ \hat{\phi}_7 \end{Bmatrix} + \begin{bmatrix} D \\ (6 \times 6) \end{bmatrix} \begin{Bmatrix} \hat{u}_1 \\ \hat{\phi}_1 \\ \hat{u}_5 \\ \hat{\phi}_5 \\ \hat{\phi}_6 \\ \hat{u}_7 \end{Bmatrix} \quad (17)$$

**Table 3** Identified model parameters of flexural beam ( $EI$  and  $\eta$ ) for the pier-girder substructure.

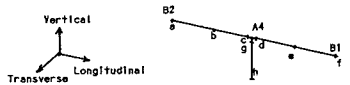
	1995-2-23 earthquake	1995-6-25 earthquake	1996-3-5 earthquake
$EI_1$	$6.75 \times 10^9$	$6.78 \times 10^9$	$5.10 \times 10^9$
$EI_2$	$1.01 \times 10^{10}$	$1.02 \times 10^{10}$	$7.70 \times 10^9$
$EI_3$	$2.59 \times 10^{10}$	$2.64 \times 10^{10}$	$2.53 \times 10^{10}$
$\zeta_1$	44.	118.	26.
$\zeta_2$	68.	180.	39.
$\zeta_3$	91.	243.	53.
Note: $EI$ ( $\text{KN-m}^2$ ) $\zeta$ (kpa-sec)			

Table 4a and Table 4b shows the retrieved maximum bending moment and shear force at each nodal point of the substructure (T-section). It

is found that significant bending moment and shear force were identified at node "g". Fig.6 and Fig.7 shows the retrieved time history of the bending moment and shear force at some of the nodal points. Comparison on the shear force time history from different seismic event at point  $h$  is shown in Fig.8. It has to be pointed out that the identified shear force at the juncture of pier and girder in transverse direction can be balanced [such as  $6190\text{kN}$  (point c) +  $10640\text{kN}$  (point d) =  $16382\text{kN}$  (point g)]. These values can be used to check with the design value of the bridge for safety evaluation.

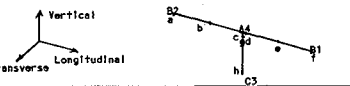
**Table 4a** Retrieved maximum bending moment at each nodal point of the pier-girder substructure (B2-A4-B1) from three earthquake loadings.

Maximum Bending Moment (KN-m)			
	1995-2-23 earthquake	1995-6-25 earthquake	1996-3-5 earthquake
a	17562	116630	15155
b	11929	78080	10515
c	19558	148830	26349
d	19558	148830	26439
e	14900	102100	17437
f	18718	169840	20629
g	170030	1124400	223851
h	0	0	0



**Table 4b** Retrieved maximum shear force at each nodal point of the pier-girder substructure (B2-A4-B1) from three earthquake loadings.

Maximum Shear Force (KN) — Transverse direction			
	1995-2-23 earthquake	1995-6-25 earthquake	1996-3-5 earthquake
a	519	3310	511
b	346	2980	232
c	798	6190	1121
d	1570	10640	2091
e	613	5250	692
f	614	5030	695
g	2318	16382	3203
h	3870	24661	4953





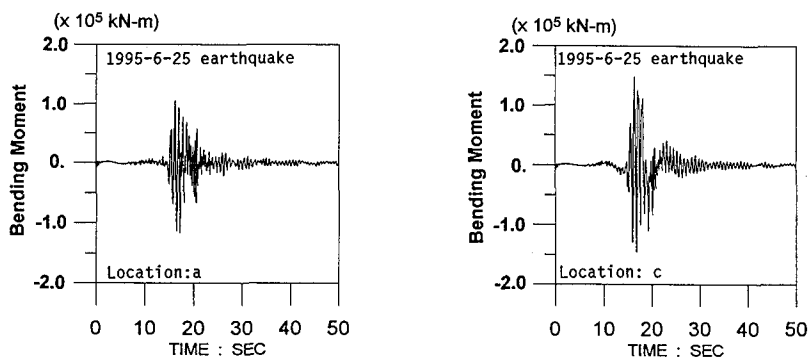


Fig.6 Retrieved time history of moment (kN-m) at nodal points of “a” and “c” for the pier-girder substructure (B2-A4-B1) during the 1995-6-25 earthquake.

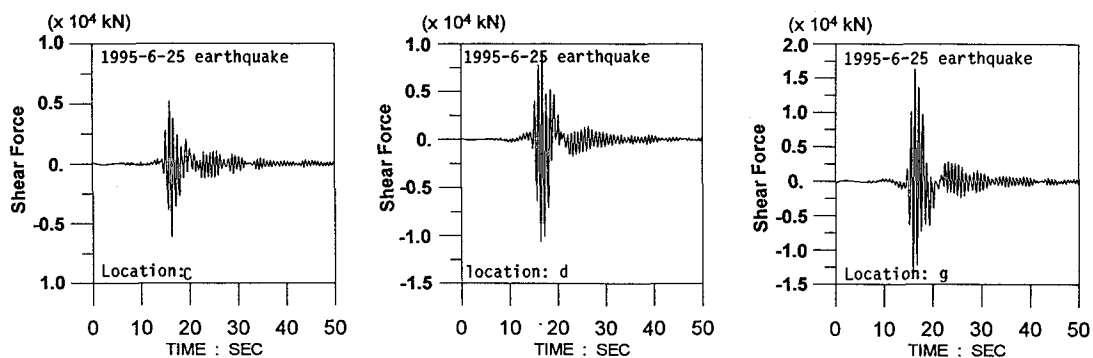


Fig.7 Retrieved time history of shear force (kN) at nodal points of “c”, “d”, and “g” for the pier-girder substructure (B2-A4-B1) during the 1995-6-25 earthquake.

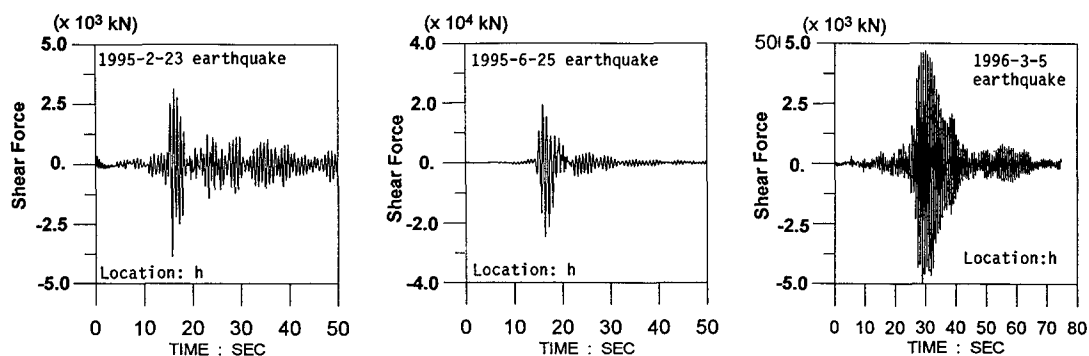
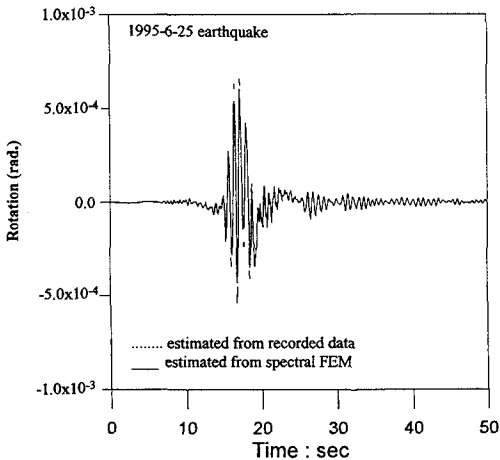


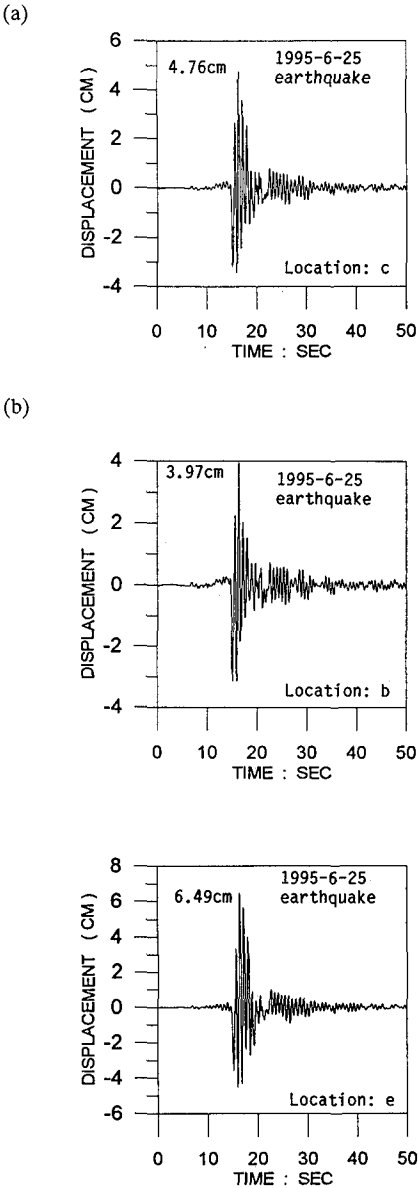
Fig.8 Comparison on the retrieved time history of shear force (kN) at nodal point “h” among three different earthquake loadings: 1995-2-23, 1995-6-25, and 1996-2-3 earthquakes, respectively.

Fig.9 shows the comparison on the rotation at node A4 (i.e.,  $\phi_3(t)$ ) between the retrieved rotation from Eq. (15) and the spline approximation from transverse motion along the deck. Good agreement between them was observed which confirm the accuracy of the proposed method. Fig.10 shows the retrieved displacement at nodes “b”, “c” and “d”. The maximum displacement is also indicated in this figure.

Next, the similar identification procedure can be applied to the bridge girder, as shown in Fig. 5(b). In this case, however, the rotational time histories at both ends of the girder are needed. The difficulty can be overcome by interpolating from the instrumental data along the deck in transverse direction. But basically speaking, the time-history of rotation at boundary nodes due to strong earthquake are more conceivable than those due to weak earthquake. In the present study only the earthquake of June 25, 1995 is considered. From the girder between two-piers A3 and A4, the identified  $EI$ -value between nodes  $d$  and  $e$  is  $9.75 \times 10^9$  and between nodes  $e$  and  $f$  is  $6.50 \times 10^9$ . It is worthy to be mentioned that the identified  $EI$ -value is consistent with the result shown in Table 3 for those of T-section from different substructure. These two different substructures, treated independently, have same result which enhance the reliability of the identification performance.



**Fig.9** Comparison on the rotation at Node A4 between retrieved rotation from spectral FEM and estimated rotation from measurements.



**Fig.10** (a) Recorded displacement at station A4 (Location c or d) in transverse direction for 1995-6-25 earthquake. (b) Retrieved displacement at location b and location e from the 1995-6-25 earthquake.

### 5. CONCLUSIONS

For the identification of bridge structure from its seismic response data the spectral finite el-

ement method was used by considering the flexural waves in beam. The dynamic stiffness of beam element was developed first. Then dynamic structural stiffness matrix of a substructure is assembled in a completely analogous way to that used for the static analysis.  $EI$ -value and  $\eta$ -value of each beam element are assumed as modal parameters. Matrix operation is performed in such a way that the interior nodal displacements of substructure can be expressed in terms of the boundary nodal displacements (it is a known displacement vector). Identification can be performed in frequency domain through such a displacement relationship. From the analysis of the seismic response data of a 5-span continuous box-girder prestressed bridge, the following conclusions are drawn:

1. The spectral element representation begins with the equation of motion of the beam which removes time from the description that the effect of damping and inertia term can be easily incorporated in the analysis. For the substructure identification the spectral element methodology provides a powerful method in the representation of dynamic problem.
2. Through matrix operation the interior nodal displacement was expressed in terms of the boundary nodal displacement of the substructure. It is convenient to choose the boundary nodes as well as part of the interior nodal displacement can be measured so that the identification formulation can be established.
3. In this example the identified  $EI$ -values of the bridge element are similar from different seismic event. This provides a health monitoring index of this bridge. The identified  $\eta$ -value (damping) increases for larger vibration response.
4. Throughout the identification, the time history of the internal member forces can be retrieved. The maximum values of the member forces during the earthquake are useful to check with the designer from the viewpoint of safety evaluation.

**ACKNOWLEDGEMENTS:** This research was founded through grants by Taiwan Area National Freeway Bureau, Ministry of Transporta-

tion and Communications, whose financial support is gratefully acknowledged. The seismic data provided by Central Weather Bureau is also acknowledged.

## REFERENCES

- 1) Cawley, P. and Adams, R. D.: "The Location of Defect in Structures from Measurements of Natural Frequencies," *J. of Strain Analysis*, 14, pp. 49-57, 1979.
- 2) Pandey, A. K., Biswas, M. and Samman, M. M.: "Damage Detection from Changes in Curvature Mode Shapes," *J. of Sound and Vibration*, 145, pp. 321-332, 1991.
- 3) Brauh, H. and Ratan, S.: "Damage Detection in Flexible Structures," *J. of Sound and Vibration*, 166, pp. 21-30, 1993.
- 4) Shinozuka, M., Yun, C. B. and Imai, H.: "Identification of Linear Structural Dynamic Systems," *J. of Engineering Mechanics*, ASCE, 108(6), pp. 1372-1390, 1982.
- 5) Hoshiya, M. and Saito, E.: "Structural Identification by Extended Kalman Filter," *J. of Engineering Mechanics*, ASCE, 110(12), pp. 1757-1770, 1984.
- 6) Hoshiya, M., Maruyama, O. and Shinozuka, J.: "Identification of Bilinear Severely Hysteretic Systems," *Proceedings of ICOSSAR 89*, Editors: Aug. Shinozuka and Schueller, pp. 1419-1425, 1989.
- 7) Naike, H. G. and Yao, J. T. P.: "System Identification of Approaches in Structural Safety Evaluation," *Structural Safety Evaluation Based on System Identification Approaches* Editors: Natke and Yao, Friedr. Vieweg and Sohn, Braunschweig/Wiesbaden, Germany, pp. 460-473, 1987.
- 8) Doyle, J. F.: *Wave Propagation in Structures: An FFT-Based Spectral Analysis Methodology*, Springer-Verlag, New York, 1989.
- 9) Chen C. C. and Liu, P. L.: "Parametric Identification of Frames Using Transient Response," *Proceedings of the 8-th Asia-Pacific Conference on Nondestructive Testing*, Taipei, December, pp. 575-582, 1995.
- 10) Loh, C. H. and Lee, Z. K.: "Seismic Monitoring of a Bridge: Assessing Dynamic Characteristics from Both Weak and Strong Ground Excitations," *Earthquake Engineering and Structural Dynamics*, 26, pp. 269-288, 1997.

(Received March 13, 1997)